

**UKAEA FUS 271**

**UKAEA Government Division**  
**Fusion**  
**(UKAEA/Euratom Fusion Association)**

**SCENE-Simulation of Self-Consistent  
Equilibria with Neoclassical Effects**

**H R Wilson**

**July 1994**

**UKAEA Government Division**  
**Fusion**

Culham, Abingdon  
Oxfordshire OX14 3DB  
United Kingdom  
Telephone 0235 463311  
Facsimile 0235 463647



# **SCENE—Simulation of Self-Consistent Equilibria with Neoclassical Effects**

**UKAEA Government Division, Fusion, Culham, Abingdon,  
Oxon, OX14 3DB, UK  
(Euratom/UKAEA Fusion Association)**

**H.R. Wilson**

**Abstract** The SCENE model for generating fixed boundary, axisymmetric equilibria with self-consistent neoclassical current profiles is described. The input and output parameters of the model are defined and their implementation in the simulation code discussed so that this report serves as a ‘user’s guide’ to the SCENE code. The description given in this report is for the version 3.0 of the code.

Fusion Theoretical and Strategic Studies Department  
Culham Laboratory  
July, 1994.



# 1 Introduction

Knowledge of current profiles in tokamaks is a very important issue for two reasons. First, there is much interest in the so-called ‘Advanced Tokamak’ designs which rely on a high percentage of bootstrap (and, at tight aspect ratio, diamagnetic) current. The bootstrap current fraction depends on the total current profile and is maximised when this is broad. Therefore an accurate prediction of the bootstrap current requires a self-consistent equilibrium, i.e. generated from the Grad-Shafranov equation in which the driving current profile contains the contribution from the bootstrap current itself. Second, there are several plasma instabilities associated with current gradients as well as micro-instabilities whose properties are influenced by the current profiles (or magnetic shear) and a model equilibrium with self-consistent current profiles is useful for studying these. These two points motivate the development of a self-consistent equilibrium simulation code in which the neoclassical effects on the current profiles are included. This report describes such a code which we have called SCENE (Self Consistent Equilibrium with Neoclassical Effects).

SCENE generates fixed boundary, axisymmetric equilibria according to a specified current profile. This can be given either as a total current profile in the plasma or as a driven current profile. The code is faster if a total current profile is specified, in which case no equilibrium iteration needs to be done for self-consistency and SCENE determines the driven current profile which would have to be supplied to obtain the specified total current. However, in reality this is not normally the case of interest. One usually has knowledge about the current which is being driven in the plasma, but the additional current resulting from bootstrap, diamagnetic and Pfirsch–Schlüter contributions depends on the equilibrium configuration and must be calculated. This dependence of the total current profile on the equilibrium leads to difficulties in generating the equilibrium: the current cannot be derived until the equilibrium is known, yet one cannot solve for the equilibrium until the current profile is known. An iterative procedure is employed in which a guess at the total current profile is made and an equilibrium generated according to this guess. The total current profile can then be calculated as the sum of the driven current and the intrinsic pressure gradient driven currents (i.e. diamagnetic, Pfirsch–Schlüter and bootstrap currents), and compared with the profile used to generate the equilibrium. In general the two will differ and so a new equilibrium is generated with this up-dated current profile. This procedure is repeated until the input current profile (i.e. that used to generate the equilibrium) matches the output profile (i.e. that calculated from the equilibrium) to some specified accuracy, when the equilibrium is then ‘self-consistent’.

The form of the driven current profile is an input to the code, to be supplied by the user. Its form will depend on the particular current drive scheme which is being modelled and may itself depend on the equilibrium and therefore be subject to the same iterative procedure described above. At present an Ohmic current drive profile is implemented. A loop voltage which is constant with radius is assumed so that the driven current profile is then governed by the conductivity. This is taken from the neoclassical calculation of Hirshman, Hawryluk and Birge (1977) and is accurate in all collisionality regimes and includes modifications due to impurity species. Neoclassical effects (i.e. due to particle trapping) are negligible in high collisionality regimes and the conductivity expression

then reduces to the classical Spitzer value. Alternatively, the driven current profile can be specified by the user, using the parameters set in the input file, to be discussed later.

In addition to the driven current, the code includes the contributions due to the three intrinsic currents: the bootstrap, Pfirsch-Schlüter and diamagnetic currents. The latter two currents are present in all collisionality regimes and can be derived using fluid theory. The diamagnetic current,  $J_{\text{dia}}$ , flows perpendicular to the magnetic field (in the flux surface) and is necessary for force balance. It is derived from

$$\mathbf{J}_{\text{dia}} \times \mathbf{B} = \nabla p \quad (1)$$

This current is not divergence free and therefore a parallel current must flow. This is the Pfirsch-Schlüter current,  $\mathbf{J}_{\text{ps}}$  which is such that

$$\nabla \cdot (\mathbf{J}_{\text{dia}} + \mathbf{J}_{\text{ps}}) = 0 \quad (2)$$

The final contribution is the bootstrap current which also flows parallel to the magnetic field but has the property that it is divergence free. The trapped particle orbits are crucial in determining the size of the bootstrap current and therefore a kinetic theory must be employed to determine its magnitude in a given tokamak equilibrium. Such a calculation has been performed by a number of authors in various limiting cases. These range from relatively simple expressions exploiting large aspect ratio expansions in the banana collisionality regime through to complex expressions which treat the full geometry and include all collisionality regimes and the effects of impurities. Most large tokamaks are in the banana collisionality regime so, in general, geometrical effects are of most interest. We therefore keep our model relatively simple and use the calculation of Hirshman (1988). This treats tokamaks of arbitrary geometry but neglects impurity effects and is restricted to the banana collisionality regime. Impurity effects can be incorporated in an approximate way as we shall describe in section 2. Also, by comparing the large aspect ratio limit of Hirshman's calculation with large aspect ratio expansions which treat all collisionality regimes, it is possible to modify Hirshman's calculation to take collisionality effects into account. Although the resulting collisionality modifications are only accurate in this large aspect ratio limit we extrapolate the results to arbitrary aspect ratio in a way similar to that described by Harris (1991). The resulting bootstrap current expression can then be applied to arbitrary aspect ratio, impure, arbitrary collisionality plasmas. This model for the bootstrap current is least reliable in tight aspect ratio plasmas with collisionality  $\nu_* \sim 1$ . It reproduces the correct result in the banana regime ( $\nu_* \ll 1$ ) and also in the fluid regime ( $\nu_* \gg 1$ ), in which case the collisional detrapping of the particles reduces the bootstrap current to zero.

In principle one could develop a fully self-consistent neoclassical equilibrium in which the plasma density and temperature profiles are governed by neoclassical particle and heat conductivities. However, there is considerable experimental evidence to suggest that both particle and heat diffusivities are 'anomalous' and are measured to be much greater than the predictions of neoclassical theory. It is therefore more relevant (in the absence of a reliable anomalous transport theory) to treat the density and temperature profiles as experimental inputs to the code. This also avoids the complexities associated with heat and particle sources. Other parameters that are required in order to construct an

equilibrium include the plasma geometry which is specified by values for the geometric major radius, aspect ratio, elongation and triangularity of the plasma. The total plasma current must be given and the vacuum toroidal magnetic field is determined by a rod current,  $I_{\text{rod}}$ , which must also be specified ( $B_{\text{vac}} = \mu_0 I_{\text{rod}} / 2\pi R$ , where  $R$  is the major radius). Unless the fully neoclassical current profile is chosen, either a total current profile or the driven current profile must be specified. Impurity information is input by giving values for the number of impurities, their charge, their central density as a fraction of the main ion species central density and their temperature and density profiles. The equilibrium can then be determined.

The remainder of the report is structured as follows. In section 2 we discuss the physics which is implemented in SCENE in more detail. Section 3 addresses the inputs to the code and discusses how to use the output to analyse the equilibrium which has been generated. Some discussion of the limitations and applicability of the model is presented in section 4 together with an example test case.

## 2 SCENE Physics

In this section we discuss the physics which is implemented in the SCENE code. There are five basic ingredients: the diamagnetic current, the Pfirsch-Schlüter current, the bootstrap current, the driven current and the resulting self-consistent Grad-Shafranov equation. In this section we consider each of these in turn.

### 2.1 Diamagnetic Current

We start with the diamagnetic current. This is determined from the force balance

$$\mathbf{J} \times \mathbf{B} = \nabla p \quad (3)$$

where  $p = p(\psi)$  is the plasma pressure, assumed constant on a flux surface, and  $\psi$  is the magnetic flux from which the magnetic field is determined:

$$\mathbf{B} = f(\psi) \nabla \phi + \nabla \psi \times \nabla \phi \quad (4)$$

Here,  $\phi$  represents the toroidal angle and  $f(\psi)$  is the toroidal field function, which is also constant on a flux surface. The toroidal field is then given by  $B_\phi = f(\psi)/R$ . The actual form of  $f(\psi)$  is determined by the rod current and the total current profile as we shall discuss later in this section. Taking the cross product of equation (3) with  $\mathbf{B}$  we obtain an expression for the diamagnetic current:

$$\mathbf{J}_{\text{dia}} = \frac{\mathbf{B} \times \nabla p}{B^2} \quad (5)$$

Using equation (4) this can be written in the form:

$$\mathbf{J}_{\text{dia}} = \frac{p'}{B^2} \left( R^2 B^2 \nabla \phi - f \mathbf{B} \right) \quad (6)$$

where a prime indicates a derivative with respect to  $\psi$ .

## 2.2 Pfirsch–Schlüter current

The diamagnetic current is perpendicular to the magnetic field and is not divergence free:

$$\nabla \cdot \mathbf{J}_{\text{dia}} = -fp'(\mathbf{B} \cdot \nabla) \left( \frac{1}{B^2} \right) \quad (7)$$

This divergence is cancelled by a parallel current, called the Pfirsch–Schlüter current. We therefore write

$$\mathbf{J}_{\text{ps}} = J_{\text{ps}} \frac{\mathbf{B}}{B} \quad (8)$$

where  $J_{\text{ps}}$  must satisfy

$$\mathbf{B} \cdot \nabla \left( \frac{J_{\text{ps}}}{B} \right) = fp'(\mathbf{B} \cdot \nabla) \left( \frac{1}{B^2} \right) \quad (9)$$

This is directly integrable and yields

$$\mathbf{J}_{\text{ps}} = \frac{fp'}{B^2} \mathbf{B} + K(\psi) \mathbf{B} \quad (10)$$

where the function  $K(\psi)$  is the ‘constant’ of integration. This arbitrary function must be deduced by considering extra physics. The charge which the diamagnetic current attempts to build up on a magnetic field line is not uniform on this field line. This leads to local electrostatic potentials and it is these which drive the Pfirsch–Schlüter current. Thus the Pfirsch–Schlüter current must obey the parallel Ohm’s law:

$$-\mathbf{B} \cdot \nabla \Phi = \eta B J_{\text{ps}} \quad (11)$$

where,  $\Phi$  is the electrostatic potential. Requiring that  $\Phi$  be single valued on the field line then provides a constraint which determines  $K(\psi)$ . Thus

$$\oint \frac{J_{\text{ps}} B}{B_\theta} dl = 0 \quad (12)$$

where  $dl$  represents the poloidal arc length element and  $B_\theta$  is the poloidal magnetic field. Defining the angled brackets by

$$\langle \dots \rangle = \frac{\oint \dots \frac{dl}{B_\theta}}{\oint \frac{dl}{B_\theta}} \quad (13)$$

we can then write down an expression for the Pfirsch–Schlüter current:

$$\mathbf{J}_{\text{ps}} = \frac{fp'}{B^2} \left( 1 - \frac{B^2}{\langle B^2 \rangle} \right) \mathbf{B} \quad (14)$$

## 2.3 Bootstrap current

The two components of the current considered above are described by fluid equations and are independent of collisionality regime. In a torus particles can become trapped in the weaker magnetic field on the outboard side and in the presence of a pressure gradient these particles have an associated current as a consequence of the finite width of their ‘banana’

orbits. This current is typically very small, but friction between the trapped and passing particles drives a much larger passing particle current: this is the so-called bootstrap current. This current relies on the presence of trapped particles and is therefore largest in low collisionality regimes, such that the trapped particles perform a bounce orbit before they experience an ‘effective’ collision (i.e. a collision which results in a de-trapping of the particle). Thus the bootstrap current is largest in the banana collisionality regime:

$$\nu_* < 1 \quad (15)$$

and is suppressed in higher collisionality regimes. In the large aspect ratio limit  $\nu_*$  is defined by

$$\nu_{*j} = \frac{\nu_j}{\epsilon \omega_{bj}} \quad (16)$$

where  $\nu_j$  is the collision frequency of the particle species, labeled by  $j$ ,  $\epsilon$  is the inverse aspect ratio and  $\omega_{bj} = \epsilon^{1/2} v_{thj}/Rq$  is the bounce frequency, with  $R$  the tokamak major radius,  $q$  the safety factor and  $v_{thj}$  the thermal velocity.

The calculation of the bootstrap current is a lengthy, involved, neoclassical theory, which has been performed by many authors in limits of large aspect ratio, differing collisionality regimes and impurity content. The original motivation for the SCENE equilibrium code was to construct self consistent tight aspect ratio equilibria; thus it is important that the bootstrap current model which is used treats finite aspect ratio effects accurately. Such a model has been derived for a two species plasma in the banana collisionality regime by Hirshman (1988) and it is this model which is incorporated in the SCENE code. Thus Hirshman calculates

$$\langle \mathbf{J}_{bs} \cdot \mathbf{B} \rangle = L_{31}^0 [A_1^e + (Z_i \tau)^{-1} (A_1^i + \alpha_i^0 A_2^i)] + L_{32}^0 A_2^e \quad (17)$$

where  $A_1^j = p'_j/p_j$ ,  $A_2^j = T'_j/T_j$  and the transport coefficients are given by

$$L_{31}^0(Z_i, x) = f(\psi)p_e x[0.754 + 2.21Z_i + Z_i^2 + x(0.348 + 1.243Z_i + Z_i^2)]/D(x) \quad (18)$$

$$L_{32}^0(Z_i, x) = -f(\psi)p_e x(0.884 + 2.074Z_i)/D(x) \quad (19)$$

$$\alpha_i^0(x) = -1.172/(1 + 0.462x) \quad (20)$$

$$D(x) = 1.414Z_i + Z_i^2 + x(0.754 + 2.657Z_i + 2Z_i^2) + x^2(0.348 + 1.243Z_i + Z_i^2) \quad (21)$$

where  $x$  is the ratio of the number of trapped to circulating particles,  $Z_i e$  is the ion charge and  $\tau$  is the ratio of electron to ion temperature. Approximate expressions for  $x$  appear in the literature which are fast to evaluate numerically. However, these are not sufficiently accurate at tight aspect ratio and in SCENE  $x = f_t/(1 - f_t)$  is calculated from the following expression:

$$f_t = 1 - \frac{3}{4}\langle B^2 \rangle \int_0^{1/B_{\max}} \frac{\lambda d\lambda}{\langle \sqrt{1 - \lambda B} \rangle} \quad (22)$$

where  $B_{\max}$  is the maximum value of the magnetic field on a flux surface.

In reality, collisionality and impurity effects can be significant and need to be taken into account. Impurities have been incorporated in a calculation by Hirshman and Sigmar (1977) and comparison between their expression and the one derived above indicates that impurities can be partially taken into account by

1. assuming quasi-neutrality:  $n_e = \sum_j n_j Z_j$  where the sum is over all ion species,  $j$ .
2. letting  $L_{31}^0(Z_i, x) \rightarrow L_{31}^0(Z_{\text{eff}}, x)$  and  $L_{32}^0(Z_i, x) \rightarrow L_{32}^0(Z_{\text{eff}}, x)$ .

This prescription differs from that suggested by Harris (1991). In particular, Harris assumes that impurities can be included by applying the transformation  $Z_i \rightarrow Z_{\text{eff}}$  wherever  $Z_i$  appears in the bootstrap current expression. However, we interpret the  $Z_i^{-1}$  factor in equation (17) as a dilution factor, representing the concentration of the main ion species. Thus, for a weak impurity concentration (such that  $n_i Z_i \gg n_z Z$  for all impurity species) this factor is unaltered. However, in the transport coefficients,  $L_{3n}$ , the prescription is that  $Z_i \rightarrow Z_{\text{eff}}$ , which can make a significant difference for high  $Z$  impurities despite the weak impurity concentration assumed. Here we define  $Z_{\text{eff}}$  by

$$Z_{\text{eff}} = \frac{\sum_j n_j Z_j^2}{n_e} \quad (23)$$

where the sum is over all ion species,  $j$ , and the subscript  $e$  labels electron quantities. Two contributions to the bootstrap current are assumed to be small and are neglected: a term resulting from the main ion-impurity ion friction is dropped and also the contribution due to impurity species pressure gradients is not included. The second approximation is justified by the weak impurity concentration, unless the impurities have strong gradients of the order  $Z/Z_i$  relative to that of the main ion species. It is more difficult to justify dropping the main-impurity ion friction term, particularly for  $Z_{\text{eff}} - Z_i \sim 1$  when our approximation may be invalid. However, at very large  $Z_{\text{eff}}$  the plasma is dominated by electrons and the bootstrap current expression is again valid.

Accepting the approximations described above, the transport coefficients can be compared with more detailed calculations which do treat impurities accurately. We compare with the model of Hirshman, Sigmar and Clarke (1976) who calculate an expression for the bootstrap current allowing for two ion species by using an approximate collision operator. Using parameters which are typical of a START equilibrium, we show this comparison as a function of  $Z_{\text{eff}}$  in figure 1 where it can be seen that good agreement is obtained over the full  $Z_{\text{eff}}$  range studied (the small discrepancy in  $L_{32}^{0e}$  is due to the approximate collision operator which has been used in the Hirshman, Sigmar, Clarke calculation).

We can also construct a model for higher collisionality regimes. For this we compare with the large aspect ratio calculation of Hinton and Hazeltine (1976) in which the bootstrap current is evaluated for arbitrary collisionality. By taking the large aspect ratio limit of equation (17) (for which  $x \simeq 1.46\epsilon^{1/2}$ ) we can identify how the transport coefficients vary with collisionality. This result can then be extrapolated to arbitrary aspect ratio to give our model for the bootstrap current:

$$\langle \mathbf{J}_{\text{bs}} \cdot \mathbf{B} \rangle = \left\{ L_{31} \frac{p'_e}{p_e} + \frac{L_{31}}{Z_i \tau} \left( \frac{p'_i}{p_i} + \alpha_i \frac{T'_i}{T_i} \right) + L_{32} \frac{T'_e}{T_e} \right\} \quad (24)$$

where we have defined

$$L_{31} = L_{31}^0(Z_{\text{eff}}, x)[1 + a_{13}\nu_{*e}^{1/2} + b_{13}\nu_{*e}]^{-1}[1 + c_{13}\tilde{\nu}_{*e}]^{-1} \quad (25)$$

$$L_{32} = [L_{32}^0(Z_{\text{eff}}, x) + (5/2)L_{31}^0(Z_{\text{eff}}, x)][1 + a_{23}\nu_{*e}^{1/2} + b_{23}\nu_{*e}]^{-1}[1 + c_{23}\tilde{\nu}_{*e}]^{-1} - (5/2)L_{31} \quad (26)$$

$$\alpha_i = \left[ \frac{\alpha_i^0 + 0.35\nu_{*i}^{1/2}}{1 + 0.7\nu_{*i}^{1/2}} + 2.1\tilde{\nu}_{*i}^2 \right] [1 + \tilde{\nu}_{*i}^2]^{-1}[1 + \tilde{\nu}_{*e}^2]^{-1} \quad (27)$$

and the coefficients are fitted functions of  $Z_i$ :

$$a_{13} = 0.027Z_i^2 - 0.211Z_i + 1.204 \quad a_{23} = 0.01Z_i^2 - 0.08Z_i + 0.64 \quad (28)$$

$$b_{13} = 0.14Z_i^2 - 0.87Z_i + 1.8 \quad b_{23} = 0.088Z_i^2 - 0.535Z_i + 1.057 \quad (29)$$

$$c_{13} = 0.097Z_i^2 - 0.67Z_i + 1.643 \quad c_{23} = 0.06Z_i^2 - 0.41Z_i + 0.96 \quad (30)$$

In the large aspect ratio calculation of Hinton and Hazeltine (1976) their definition of collisionality varies with major radius and is not constant on a flux surface at finite aspect ratio. We therefore require a more general definition of collisionality. Mathematically,  $\nu_* \sim 1$  corresponds to the balance

$$B_\theta \frac{\partial f}{\partial l} \sim \frac{\nu_j}{v^2} v \frac{\partial}{\partial \lambda} \left[ \lambda(1 - \lambda B)^{1/2} \right] \frac{\partial f}{\partial \lambda} \quad (31)$$

in the kinetic equation, where  $l$  is the poloidal arc length and  $\lambda$  is the pitch angle variable. Averaging over the particle velocity,  $v$ , and recognising that for trapped particles we have  $\lambda \sim 1/B_{\max}$  (where  $B_{\max}$  is the maximum value of the magnetic field on the flux surface under consideration) and  $\Delta\lambda \sim 1/B_{\min} - 1/B_{\max}$  (where  $\Delta\lambda$  is the change in  $\lambda$  between passing and trapped orbits) then leads to the balance

$$1 \sim \frac{\nu_j}{v_{thj}} \left[ \frac{B_{\max} + B_{\min}}{B_{\max} - B_{\min}} \right]^2 B_{\max} \oint \left[ 1 - \frac{B}{B_{\max}} \right]^{1/2} \frac{dl}{B_\theta} \quad (32)$$

Normalising with respect to the large aspect ratio definition given by Hinton and Hazeltine (1976) we obtain the expression for the collisionality which we use in our bootstrap current expression:

$$\nu_{*j} = \frac{\nu_j}{4v_{thj}} \left[ \frac{B_{\max} + B_{\min}}{B_{\max} - B_{\min}} \right]^2 B_{\max} \oint \left[ 1 - \frac{B}{B_{\max}} \right]^{1/2} \frac{dl}{B_\theta} \quad (33)$$

where the collision frequencies for the electrons and main ion species are defined by

$$\nu_e = \frac{1}{3(2\pi)^{3/2}\epsilon_0^2} \frac{n_i Z_i^2 e^4 \ln \Lambda}{m_e^{1/2} (k_B T_e)^{3/2}} \quad \nu_i = \frac{1}{3\sqrt{2}(2\pi)^{3/2}\epsilon_0^2} \frac{n_i Z_i^4 e^4 \ln \Lambda}{m_i^{1/2} (k_B T_i)^{3/2}} \quad (34)$$

Similar considerations for the passing particles leads to a general aspect ratio result for  $\epsilon^{3/2}\nu_{*j}$  which we represent by  $\tilde{\nu}_{*j}$ :

$$\tilde{\nu}_{*j} = \frac{\sqrt{2}}{2\pi} \frac{\nu_j}{v_{thj}} B_{\max} \oint \frac{dl}{B_\theta} \quad (35)$$

Using the facts that the bootstrap current flows parallel to the magnetic field and that it is divergence free, one can show that it must take the form

$$\mathbf{J}_{\text{bs}} = \frac{\langle \mathbf{J}_{\text{bs}} \cdot \mathbf{B} \rangle}{\langle B^2 \rangle} \mathbf{B} \quad (36)$$

This completes our description of the intrinsic currents (i.e. those driven by the pressure gradients which exist in the plasma) which are implemented in the SCENE model.

## 2.4 Driven current

The final contribution is the externally driven current which is assumed to be divergence free and parallel to the magnetic field; thus it is of the form:

$$\mathbf{J}_{\text{ext}} = \frac{\langle \mathbf{J}_{\text{ext}} \cdot \mathbf{B} \rangle}{\langle B^2 \rangle} \mathbf{B} \quad (37)$$

The profile  $\langle \mathbf{J}_{\text{ext}} \cdot \mathbf{B} \rangle$  is, in general, to be specified by the user and will depend on the current drive mechanism which is assumed. However, the code does have an ‘Ohmic’ option in which all the externally driven current is assumed to be induced by transformer action. If this option is selected then  $\mathbf{J}_{\text{ext}}$  is calculated using the formula

$$\mathbf{J}_{\text{ext}} = \sigma_{\text{nc}} \frac{\langle \mathbf{E} \cdot \mathbf{B} \rangle}{\langle B^2 \rangle} \mathbf{B} \quad (38)$$

where the driving electric field is assumed to be in the toroidal direction and can be written in terms of the loop voltage,  $V$

$$\mathbf{E} = \frac{V}{2\pi R} \mathbf{e}_\phi \quad (39)$$

where  $\mathbf{e}_\phi$  is a unit vector in the toroidal direction and  $R$  is the major radius of the point of interest in the tokamak plasma. The neoclassical conductivity which is used in the code is the result of Hirshman, Hawryluk and Birge (1977):

$$\frac{\sigma_{\text{nc}}}{\sigma_0} = \frac{8}{3\sqrt{\pi}} \int_0^\infty y^4 e^{-y^2} dy \left( (1 - f_t^*) F_s [1 - f_t^* (\nu_D^e \tau_{ee} F_s - 1)] \right) \quad (40)$$

where  $\sigma_0 = n_e e^2 \tau_{ee} / m_e$ ,  $\tau_{ee} = 3(4\pi\epsilon_0)^2 m_e^2 v_{the}^3 / (16\sqrt{\pi} n_e e^4 \ln \Lambda)$  and

$$\nu_D^e(y) = \left( \frac{4}{3\sqrt{\pi}} \tau_{ee} \right)^{-1} \left( \frac{\Phi(y) - G(y) + Z_{\text{eff}}}{y^3} \right) \quad (41)$$

$\Phi$  and  $G$  are the error function and Chandrasekhar function:

$$\Phi(y) = \left( \frac{2}{\sqrt{\pi}} \right) \int_0^y e^{-t^2} dt \quad G(y) = \frac{\Phi(y) - y\Phi'(y)}{2y^2} \quad (42)$$

and  $f_t^*$  is the effective trapped particle fraction in the presence of collisions:

$$f_t^* = f_t (1 + 1.75 \nu_{*e} [\nu_D^e(y) \tau_{ee}] y^{-1})^{-1} \quad (43)$$

where  $f_t$  is the trapped particle fraction in the absence of collisions (given by equation (22)). Note that the collisionality parameter used here is defined differently to that used in the bootstrap current calculation. The definition used by Hirshman, Hawryluk and Birge is  $\nu_{*e} = \sqrt{2}\epsilon^{-3/2}R_0q/(v_{the}\tau_{ee})$ . The Spitzer function,  $F_s(Z_{\text{eff}}, y)$  is fitted to a polynomial:

$$F_s(Z_{\text{eff}}, y) = \Lambda_E(Z_{\text{eff}}) - \Lambda_T(Z_{\text{eff}})L_1(y^2) + \frac{8}{15} \left( \frac{1}{Z_{\text{eff}}} - \Lambda_E(Z_{\text{eff}}) + \frac{3}{2}\Lambda_T(Z_{\text{eff}}) \right) L_2(y^2) \quad (44)$$

where

$$\Lambda_E(Z_{\text{eff}}) = \frac{3.40}{Z_{\text{eff}}} \left( \frac{1.13 + Z_{\text{eff}}}{2.67 + Z_{\text{eff}}} \right) \quad (45)$$

$$\Lambda_T(Z_{\text{eff}}) = 2.06 \left( \frac{1.38 + Z_{\text{eff}}}{3.23 + 4.68Z_{\text{eff}} + Z_{\text{eff}}^2} \right) \quad (46)$$

$$L_1(y^2) = \frac{5}{2} - y^2 \quad (47)$$

$$L_2(y^2) = \frac{35}{8} - \frac{7}{2}y^2 + \frac{1}{2}y^4 \quad (48)$$

We now combine the four components to derive the following expression for the total current profile in a tokamak:

$$\mathbf{J} = \frac{\langle \mathbf{J}_{\text{ext}} \cdot \mathbf{B} \rangle}{\langle B^2 \rangle} \mathbf{B} + \frac{\langle \mathbf{J}_{\text{bs}} \cdot \mathbf{B} \rangle}{\langle B^2 \rangle} \mathbf{B} + p' \left( R^2 \nabla \phi - \frac{f}{\langle B^2 \rangle} \mathbf{B} \right) \quad (49)$$

where the last term is the combination of the diamagnetic and Pfirsch-Schlüter currents.

## 2.5 Equilibrium solution

In order to evaluate the various flux surface averages required to determine this total current we must next solve the Grad-Shafranov equation for the equilibrium:

$$\Delta^* \psi = -\mu_0 \left( R^2 p' + \frac{ff'}{\mu_0} \right) \quad (50)$$

where primes indicate differentials with respect to the poloidal flux,  $\psi$ . The pressure profile  $p(\psi)$  is determined, in principle, by heat and particle sources and transport processes in the plasma. No reliable theory exists for these at present and instead we treat the pressure profile as an input to the model, to be provided by experimental measurements. The toroidal field function,  $f(\psi) = RB_\phi$  is related to the current profile and therefore cannot be treated as free if the equilibrium is to be solved for in a self-consistent manner. In particular, making use of force balance and Ampère's law allows the total current profile to be written as

$$\mathbf{J} = R^2 p' \nabla \phi + \frac{f' \mathbf{B}}{\mu_0} \quad (51)$$

so that, making use of equation (49) we can determine  $f(\psi)$  from:

$$\frac{ff'}{\mu_0} = \frac{\langle \mathbf{J}_{\text{ext}} \cdot \mathbf{B} \rangle}{\langle B^2 \rangle} f + \frac{\langle \mathbf{J}_{\text{bs}} \cdot \mathbf{B} \rangle}{\langle B^2 \rangle} f - \frac{f^2 p'}{\langle B^2 \rangle} \quad (52)$$

To calculate the self-consistent equilibrium equations (50) and (52) must be solved simultaneously: this is the objective of the SCENE code. In order to derive the solution the following iterative procedure is employed. First an initial guess at the  $f(\psi)$  profile is made and equation (50) solved for the equilibrium. This equilibrium is then used to evaluate the right hand side of equation (52) and compared with the value of  $ff'$  used to calculate the equilibrium. In general these will differ so  $ff'$  is re-defined according to equation (52) and a new equilibrium evaluated. This procedure is repeated until the  $ff'$  profile used to generate the equilibrium equals the right hand side of equation (52) to within some specified accuracy. This convergence is usually very rapid (if, indeed, it does converge) and three or four equilibrium iterations are generally sufficient. Convergence is most rapid when the toroidal field is dominated by its vacuum value, for then  $f(\psi)$  is dominated by a large constant term and the right hand side of equation (52) does not vary significantly with different  $ff'$  profiles. If this is not the case then difficulty may be experienced in obtaining convergence.

### 3 Input and Output Specification and Error Information

In this section we describe the inputs and outputs of the SCENE code. A flow chart of the internal structure is given in the Appendix.

#### 3.1 Input specification

Here we describe the input data required for the equilibrium generation and also how to gain access to the diagnostic results which are performed on the final, converged equilibrium. The input is read in by SCENE in free format from the file unit NREAD. This file is of the form:

```
NREAD    NW
IGR
TITLE
'VAR1'  VAL1
'VAR2'  VAL2
...
'FINI'  1
```

NREAD and NW are integers defining the read and write units to be used. If GHOST graphics (Prior (1993)) is available SCENE has some graphics diagnostics which can be switched on by setting IGR> 0 as follows:

IGR	Description
0	No graphs plotted
1	plots plasma profiles only
2	as 1 but also plots flux contours
3	as 2 but also plots $ B $ contours
4	as 3 but no flux contours

The title of the particular run is input by **TITLE** which can handle nineteen characters. Then follows a list of the inputs required by **SCENE**. These are in the form of a four-character string representing the variable followed by the value to which that variable must be set. If a variable name is not specified its default value (set in the routine **DEFAULT**) is used. The key for the parameter strings and their default values are described in table 1. The command '**FINI**' signifies the end of the data file for a pure plasma (i.e. occurs at the end of the parameter list shown in table 1). If the plasma is impure, (indicated by the parameter **IMP=1**, set in the upper part of the data file) then the impurity data should be included in the input file immediately following the **FINI** command. This is in the format:

**NIMP**

**IZ(I+1) ZN(I+1) ZT(I+1) ZAT(I+1) ZAN(I+1)**

where **NIMP** specifies the number of impurity species. There then follows **NIMP** rows of arrays which give the impurity ion charge, fraction of the impurity ion relative to main species (at the plasma centre), central temperature,  $\alpha_T$  (where the temperature profile  $\sim (1 - x)^{\alpha_T}$ ) and  $\alpha_n$  (where the density profile  $\sim (1 - x)^{\alpha_n}$ ). These are stored in the arrays in the elements 2 through to **NIMP+1** and the first element is reserved for the main ion species properties (defined in the upper part of the data file). We have defined  $x = 1 - \psi/\psi_0$  where  $\psi_0$  is the value of  $\psi$  on axis (note that  $\psi = \psi_0$  is maximum on axis and zero at the plasma boundary).

## 3.2 Output specification

We now discuss the diagnostic output that can be obtained from **SCENE**. When **SCENE** detects that the  $ff'$  profile has converged it calls the subroutine **OUTPUT** in which various diagnostic calculations are performed and (if a graphics package is attached) calls to the graphics routines are made. The diagnostics are stored in common blocks which can be accessed in the user routine **USRCAL**. The definitions are described in the following subsections. All lengths are in m, temperature in eV, current in A and magnetic field in T.

### 3.2.1 Flux surface averaged quantities

These are stored in the common block **AVGES**. Each quantity is stored as a one dimensional array of the form **VAR(I)** where  $1 \leq I \leq NCON + 1$ , and **NCON** is the number of

flux surfaces specified in the input file. The properties of a flux surface are stored in the common block FLXVAR as follows

**FLXR(I,J)** Stores the  $R$  coordinates of points around each of the flux surfaces labelled by I for  $1 \leq I \leq NCON+1$ . The label J is in the range  $1 \leq J \leq ICON(I)$ .

**FLXZ(I,J)** Same as FLXR but gives the  $Z$  coordinates of the points.

**EPS(I)** Stores the inverse aspect ratio of flux surface I

**SIST(I)** Stores the value of poloidal flux on the flux surface I. SIST corresponds to a definition such that  $\psi$  is a maximum at the magnetic axis and is zero at the plasma boundary.

**ICON(I)** Stores the number of points on the flux surface I.

**NCON** Stores the number of flux surfaces calculated.

The flux surface averaged quantities that have been calculated on these flux surfaces are then in the common block AVGES and stored in the following arrays

**SFAC(I)** Safety factor on the flux surface I

**BSQAV(I)**  $\langle B^2 \rangle$

**RSQAV(I)**  $\langle R^2 \rangle$

**RINV(I)**  $\langle R^{-1} \rangle$

**RSQINV(I)**  $\langle R^{-2} \rangle$

**RAV(I)**  $\langle R \rangle$

**RNORM(I)**  $\oint B_\theta^{-1} dl$

**FTRAP(I)** Banana regime trapped particle fraction.

**BSJ(I)**  $\frac{\langle \mathbf{J}_{bs} \cdot \mathbf{B} \rangle}{\langle B^2 \rangle^{1/2}}$

### 3.2.2 Global quantities

Global quantities are stored in the common block BETVAL as follows

AREA	Cross sectional area of plasma
BETA	$\beta = 200\mu_0 \frac{\oint p dV}{\oint B^2 dV} \%$
BETAI	$\frac{8\pi \oint p dA}{\mu_0 I_p^2}$
BETAP	$\frac{2\mu_0 \oint p dV}{\oint B_\theta^2 dV}$
AVEL	Volume averaged electron density
AVT	Volume averaged electron temperature
BETLIM	$3.5 \times 10^{-6} \frac{I_p}{AB_v}$ , $A$ =aspect ratio, $B_v$ =vacuum toroidal field at geometric axis.
CONFT	Confinement time = $1.5 \frac{\oint p dV}{VI_p}$ , $V$ =loop volts
RLI	Internal inductance = $2 \frac{\oint B_\theta^2 dV}{\mu_0^2 I_p^2 R_0}$ , $R_0$ =magnetic axis radius

The total toroidal current contributions are stored in the common block TOTCUR as follows:

TOTBS	bootstrap current
TOTPS	Pfirsch-Schlüter current
TOTDI	diamagnetic current
TOTEX	driven current
TOTGS	total current
VLOOP	loop volts (if NEO=1 or -1)
VNOBS	loop volts if $J_{bs} = 0$ (if NEO=1 or -1)
VSPIT	Spitzer loop volts (if NEO=1 or -1)

Other global parameters are those of the plasma cross-section shape, stored in common block PARAM

RCEN	geometric axis
TOKEPS	inverse aspect ratio
ELON	elongation
TRI	triangularity

### 3.2.3 Local quantities

Local quantities are stored on a square mesh whose coordinates are stored in the common block MESH in  $R(I)$  and  $Z(J)$ . The labels I and J are in the range  $1 \leq I \leq NR$  and  $1 \leq J \leq NZ$  where NR and NZ are also stored in MESH. The toroidal components of the current profiles are stored in the common block CURE in two-dimensional arrays such that VAR(I,J) is its value at  $R=R(I)$ ,  $Z=Z(J)$ :

BSPH(I,J)	bootstrap current density profile
PSPH(I,J)	Pfirsch-Schlüter current density profile
DIPH(I,J)	diamagnetic current density profile
EXPH(I,J)	externally driven current density profile
GRADJ(I,J)	total current density profile

The value of  $\psi$  on each of these mesh points is stored in the variable U(I,J) and is passed as an argument into subroutine USRCAL. The definition of  $\psi$  used in U is the same as that for SIST, i.e. maximum on axis and zero at the plasma boundary. Knowing  $\psi$  at each point then allows temperature, pressure and toroidal field function profiles to be determined by calling the relevant function. For the electron temperature this is TEMPE(PSI, ID), for the ion temperature TEMP1(PSI, K, ID) and for the total pressure PRESS(PSI, ID). In each case PSI is the flux (value of U), and for ID=0 (or ID=1) the parameter (or its derivative with respect to  $\psi$ ) is returned. For the ion temperature, K=1 labels the main ion while other values of K correspond to the impurities (in the order in which they are listed at the end of the input file). If no impurities are present (IMP=0) the electron and ion densities must be constructed from the pressure and temperatures. If impurities are present (IMP=0) the electron density is calculated by a call to DENSE(PSI, ID) and the ions by DENSI(PSI, K, ID). The toroidal field function,  $f(\psi)$ , and its derivatives are obtained by a call to the function FPROF(PSI, ID) where again PSI is the poloidal flux. ID = 1 returns  $ff'$ , ID = 2 returns  $f$  and ID=3 returns  $f'$  where derivatives are with respect to  $\psi$ . The integer array IXOUT(I,J) which is passed as an argument into USRCAL determines the region of mesh occupied by plasma; mesh points with IXOUT(I,J)=1 are inside the plasma and all other values are outside.

Note that local values of the poloidal field are stored in the array BTHETA(I,J) but these are calculated on a different mesh to that of the currents. In particular, BTHETA(I,J) corresponds to the value of  $B_\theta$  at  $R = \text{RCOORD}(I)$ ,  $Z = \text{ZCOORD}(J)$ . The number of elements in the  $R$  and  $Z$  direction is NR and NZ as for the previous mesh, but other properties are different and are stored in the common block BMESH.

### 3.3 Error messages

SCENE has several error indicators. The error is described before the calculation is terminated and the routine in the code where the error has been detected is given. There are two main reasons for an error. First, the user may have used the continuation facility (i.e. set ICON=-1) while the equilibrium being generated is defined on a different mesh to that which is stored in the unit 7 (see description of ICON input parameter in table 1 for more details). If in doubt ICON=1 should be used. The second reason for an error is that the equilibrium has not converged to sufficient accuracy. The user should set IPR=0 in the input file (so that the equilibrium iteration can be followed interactively by the user) and check that the maximum number of allowed iterations (set in NOUT) is not reached. Convergence properties may be improved by varying the OMEG and FRAC parameters, or increasing NOUT.

## 4 Example Test Case and Model Validity

In this section we give an example input file and corresponding graphical output produced by SCENE. The input file is given in table 2 and represents an Ohmic START discharge with a neoclassical conductivity profile assumed. A high density has been chosen to enhance the effects of collisionality. In this case three impurity species are included with temperature and density profiles which match the main ion species. The collisionality model has been used in both the bootstrap current expression and the conductivity profile. The graphical output is illustrated in figure 2. The first page (figure 2a) shows the flux surface contours, with bold contours representing the approximate positions of the  $q = 1$  and  $q = 2$  surfaces (note that no  $q = 1$  surface exists in this example). The column of numbers on the right of the figure are the values of  $q$  on each of the flux surfaces drawn. The second page (figure 2b) shows plots of the density and temperature profiles, collisionality profile (note that impurity effects are not included in the definition of collisionality here), the toroidal magnetic field (the dashed line is the vacuum value) and the safety factor. A summary of the input parameters is provided at the top of the figure and a list of diagnostic parameters is given on the right (these have the same definitions as the variables described in section 3.2). Finally the third page of figures (figure 2c) illustrates the current profiles across the tokamak mid-plane. Information related to the current profiles and plasma boundary shape is given on the right of the figure. It is interesting to note that the predicted loop volts of 2V is in agreement with START measurements, thus providing some support for the model. Note also the collisional broadening of the total current profile. In the absence of collisions, neoclassical theory predicts a very ‘spiked’ current profile as a result of its  $\epsilon^{1/2}$  dependence (where  $\epsilon$  is the inverse aspect ratio). Collisions will tend to detrap particles and so lead to the much rounder profile shown in figure 2c.

To conclude this report we discuss some of the approximations used and how they are expected to affect the results. From the discussion given in section 2, the model is clearly most valid in a low collisionality ( $\nu_* \ll 0.1$ ), pure plasma. The approximate impurity model which has been incorporated in the bootstrap current expression is not expected to have large errors, particularly if a large part of the current is driven by the electron density and temperature gradients (i.e. the electron pressure exceeds the ion pressure). The collisionality model which is incorporated in the conductivity expression is expected to be good in all parameter regimes. However, the collisionality model employed in the bootstrap current expression is strictly valid only in the large aspect ratio limit (or near the magnetic axis of a tight aspect ratio device) and the result has been extrapolated to arbitrary aspect ratio. Caution should therefore be used in interpreting the results for a high collisionality tight aspect ratio plasma which has a large bootstrap current fraction. We note also that impurity effects are not included in the calculation of the collisionality effects on the bootstrap current, nor in the collisionality plot produced by the graphical output. Because of the peaked nature of the neoclassical conductivity profile, one sometimes finds that the safety factor on axis drops below unity. In a tokamak, the current profile is often modified through sawtooth activity at the centre, in order to prevent  $q$  dropping significantly below unity. At present SCENE has no sawtooth model and such cases cannot be simulated. Realistic equilibria, therefore should not have a

central  $q$  which falls significantly below unity.

**Acknowledgements** I should like to thank J W Connor and R J Hastie for many useful discussions. This work was funded jointly by the UK Department of Trade and Industry and Euratom.

## REFERENCES

- Harris G.R. (1991) Euratom-CEA Report EUR-CEA-FC-1436
- Hinton F.L. and Hazeltine R.D. (1976) Rev.Mod.Phys. **48** 239
- Hirshman S.P. Sigmar D.J. and Clarke J.F. (1976) Phys.Fluids **19** 656
- Hirshman S.P. and Sigmar D.J. (1977) Phys.Fluids **20** 418
- Hirshman S.P. Hawryluk R.J. and Birge B. (1977) Nucl.Fus. **17** 611
- Hirshman S.P. (1988) Phys.Fluids **31** 3150
- Prior W.A.J. (1993) ‘GHOST Graphical Output System User Manual’, Version 9.0, (AEA Technology, Culham), (ISBN 0 85311 186 3)

## FIGURE CAPTIONS

- Figure 1:** Comparison of Hirshman (1988) transport coefficients with  $Z \rightarrow Z_{\text{eff}}$  with the two ion species model of Hirshman, Sigmar and Clarke (1976)
- Figure 2:** Graphical output produced by SCENE showing the flux surface contours (a), some plasma profiles (b) and the current profiles (c).



## Appendix - SCENE code structure

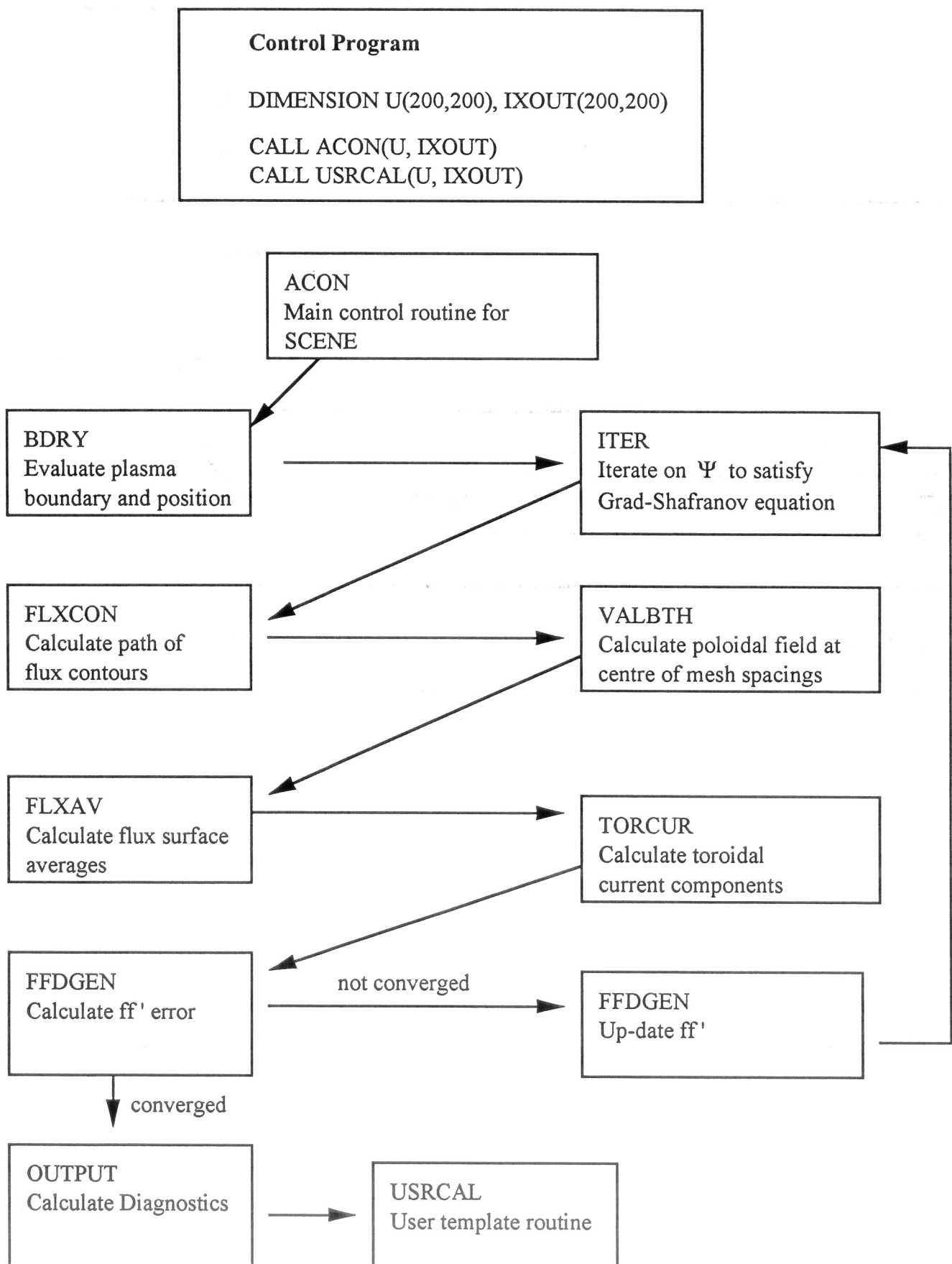


**Table 1: Parameters required by SCENE to evaluate bootstrap current and conductivity profile.**

Variable	Default	Description
'RCEN'	0.2	Geometric axis of plasma boundary (in m)
'EPS'	0.9	Inverse aspect ratio of plasma boundary
'ELON'	1.3	Elongation of plasma boundary
'TRI'	0.3	Triangularity of plasma boundary
'STEP'	0.01	Sets the spacing for the square mesh used by SCENE, which is assumed to be equal in both the $R$ and $Z$ directions.
'IPR'	0	Prints out array indicating plasma position in the square mesh if set to 1
'PPOW'	2	For a pure plasma this parameterises the electron pressure gradient profile by $p'_e(x) \sim (1 - x)^{\alpha_p}$ , where $\alpha_p$ is PPOW and $x$ is the normalised poloidal flux, $x = 1 - \psi/\psi_0$ with $\psi_0$ the value on axis (note $\psi = 0$ at the edge). If impurities are present (i.e. IMP=1) then this parameterises the main ion density profile by $n_i \sim (1 - x)^{\alpha_p}$ . The electron density is then determined from this and the impurity density information input at the end of the data file (see sub-section 3.1 for description).
'FPOW'	0.1	The definition of this variable depends on the type of equilibrium to be generated. If one wishes to specify a total current profile, (indicated by ITOT=1) then the equilibrium is generated with $ff' = (1 - x)^{\alpha_f}$ where $\alpha_f$ is FPOW. Alternatively, if one wishes to specify the applied current profile then $ff'$ is to be calculated and this profile is used as the first guess. FPOW may also be used to parameterise the applied current profile if the neoclassical or classical Ohmic current profiles are not selected (NEO=0)—this parameterisation is defined in the description of POWJ.
'TPOE'	0.8	Electron temperature profile parameterisation, $T(x) = T_{0e}(1 - x)^{\alpha_{Te}}$ where $\alpha_{Te}$ is TPOE.
'TPOI'	0.8	Ion temperature profile parameterisation, $T(x) = T_{0i}(1 - x)^{\alpha_{Ti}}$ where $\alpha_{Ti}$ is TPOI.

**Table 1: Parameters required by SCENE to evaluate bootstrap current and conductivity profile (cont).**

Variable	Default	Description
'TOE'	180	Peak electron temperature in eV (i.e. $T_{0e}$ )
'TOI'	150	Peak ion temperature in eV (i.e. $T_{0i}$ )
'CUR'	0.1	Total plasma current in MA (positive current definition and converted to A in the code)
'BPOL'	0.8	Measure of poloidal beta (scales $p'$ relative to $ff'$ )
'BPFA'	1.0	Extra enhancement factor on pressure; used to gain very high beta equilibria
'RODI'	0.05	Rod current (in MA); proportional to vacuum toroidal magnetic field, $B_{\text{vac}} = \mu_0 I_{\text{rod}} / 2\pi R$ (converted to A in the code)
'ZM'	1	Charge of main species ion
'IMP'	0	Switch to indicate pure plasma ( <b>IMP=0</b> ) or impure plasma ( <b>IMP=1</b> ). Note, if the impure plasma option is selected the impurity properties must be input in the lines of data following the ' <b>FINI</b> ' command (see section 3).
'NEO'	1	If <b>NEO</b> = ±1 then any input value of <b>ITOT</b> is over-ridden and <b>ITOT</b> is set to zero. For <b>NEO</b> =1 the driven current profile is derived from the neoclassical conductivity profile and a constant loop voltage is assumed. For <b>NEO</b> =-1 a classical conductivity profile is assumed. For <b>NEO</b> =0 then, if <b>ITOT</b> =0 the applied current profile is parameterised as described under <b>POWJ</b> . Alternatively, if <b>ITOT</b> =1 the total current profile is specified through the function $ff'$ and pressure profile.

**Table 1: Parameters required by SCENE to evaluate bootstrap current and conductivity profile (cont).**

Variable	Default	Description
'POWJ'	1	If NEO=0 and ITOT=0 then the user must define the current profile by setting POWJ. Defining $\alpha_J = \text{POWJ}$ the driven current profile is parameterised as
		$\frac{\langle J \cdot B \rangle}{\langle B^2 \rangle} = J_0(1 - x^{\alpha_J})^{\alpha_f}$
		where $\alpha_f$ is FPOW, which is also used to parameterise the initial guess for the $ff'$ profile (see description under FPOW).
'NCO'	0	If set to zero collisional effects on the trapped particle fraction are not included. If set to 1 then a collisional model is employed for both the bootstrap current and the neoclassical conductivity profile. If set to 2 then collisional effects are not included in the bootstrap current calculation but are retained in the neoclassical conductivity.
'ITOT'	0	This parameter is set to 1 if the user wishes to specify the total current profile (i.e. driven + b/strap + diamag + P/S) or zero if the user wishes to specify the driven current profile. If ITOT=1 then the $ff'$ profile is that specified in the description of FPOW and SCENE derives the various contributions to this total current. If ITOT=0 then the $ff'$ profile specified is a first guess at the $ff'$ required. In this case the equilibrium is iterated until the $ff'$ used to generate the equilibrium is consistent with the total current profile evaluated by SCENE.
'NCON'	15	Defines the number of flux surfaces used to construct the $ff'$ profile. These are approximately evenly spaced in aspect ratio.
'NOUT'	120	Defines the maximum number of ‘outer’ iterations allowed in which to converge one equilibrium for a given $ff'$ guess.
'NINN'	4	Defines the maximum number of ‘inner’ iterations allowed between outer iterations during the calculation of an equilibrium for a given $ff'$ guess.

**Table 1: Parameters required by SCENE to evaluate bootstrap current and conductivity profile (cont).**

Variable	Default	Description
'NPAS'	10	Defines the maximum number of equilibrium iterations allowed in which to converge the $ff'$ profile (if ITOT=0)
'ERIT'	0.001	Error to be tolerated in the Grad-Shafranov solver
'ERFD'	0.01	Maximum error to be tolerated in the ‘converged’ $ff'$ profile (if ITOT=0)
'OMEG'	1.6	Varying this parameter may help speed up the convergence of the Grad-Shafranov solution; however some values may give rise to difficulties in obtaining a converged solution
'FRAC'	0.1	Varying this parameter may help speed up the convergence of the Grad-Shafranov solution; however some values may give rise to difficulties in obtaining a converged solution
'ICON'	1	When the equilibrium for the initial $ff'$ guess has converged, its properties are written into the file unit 7. This allows a rapid re-calculation of similar equilibria, using this stored equilibrium as an initial guess. If no equilibrium is stored, or if the mesh properties of the equilibrium to be calculated differ from that stored, then ICON=1 must be set. However, if a similar equilibrium to that stored (i.e. the last one calculated by SCENE) is to be calculated on the <i>same</i> mesh then setting ICON=-1 allows the stored equilibrium to be used as an initial guess, and so speeds up the calculation. A word of warning—the most common cause for an error being detected in the equilibrium generation or analysis is as a result of the user setting ICON=-1 but at the same time trying to generate an equilibrium on a different mesh to that stored in file unit 7.
'FINI'		Indicates the end of this section of the data file (must be included). The impurity ion data follows this as described in section 3.1

Table 2: Input data file for SCENE 3.0 test case.

```

11 6          read/write units (nb change value of NREAD in code)
2            > 0 to switch on graphics
SCENE 3.0 Test Case           job title
'RCEN'  0.165      Geometric axis of plasma boundary (m)
'EPS '  0.697      Inverse aspect ratio of boundary
'ELON'  1.3        Elongation of plasma boundary
'TRI '  0.3        Triangularity of plasma boundary
'STEP'  0.005      Mesh size (m)
'IPR '  0          Controls amount of printout
'PPOW'  0.8        p_e' profile (or main ion density profile if IMP=1)
'FPOW'  2.0        initial ff' profile
'TPOE'  0.8        electron temperature profile
'TPOI'  0.8        ion temperature profile
'POWJ'  1.0        current profile (unless NEO=1)
'TOE '  180.       Central electron temperature (eV)
'TOI '  150.       Central ion temperature (eV)
'CUR '  0.065      total toroidal plasma current (MA)
'BPOL'  0.7        approx poloidal beta
'BPFA'  1.          pressure enhancement factor
'RODI'  0.48       rod current (gives vacuum B-field) (MA)
'ZM '   1.          Charge of main species ion (<ZEFF)
'IMP '  1           =1 (0) for (no) impurities
'NEO '  1           =1 (0) for neo. (user) current, --1 for class.
'NCO '  1           =1 for collisionality model
'ITOT'  0           =1 (0) to set total (applied) current profile
'S   '  1.0E8       Guess at current scaling
'OMEG'  1.6         accelerates equilibrium convergence (prop. to psi)
'FRAC'  0.1         maximises acceleration
'NCON'  20          number of flux surfaces evaluated
'NOUT'  100         no. iter. in G-S eqn. solver
'NINN'  4           no. inner iter. in G-S eqn. solver
'NPAS'  10          max number of equil. iterations
'ERIT'  0.0001     error used for G-S eqn solution
'ERFD'  0.01        error between input and output currents
'ICON'  +1          -1 (+1) to use old (restart new) eqbm. in 1st iter.
'FINI'  1           Indicates end of data file (must be at end of file)
3             Number of impurity ions
6 0.018 150 0.8 0.8    z,n,T,at,an
5 0.023 150 0.8 0.8    z,n,T,at,an
10 0.001 150 0.8 0.8   z,n,T,at,an

```

Figure 1

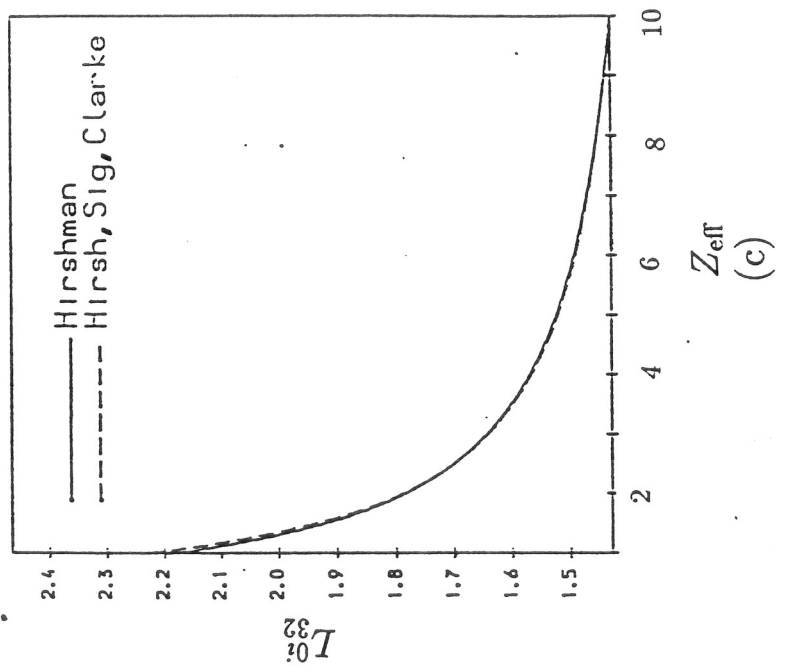
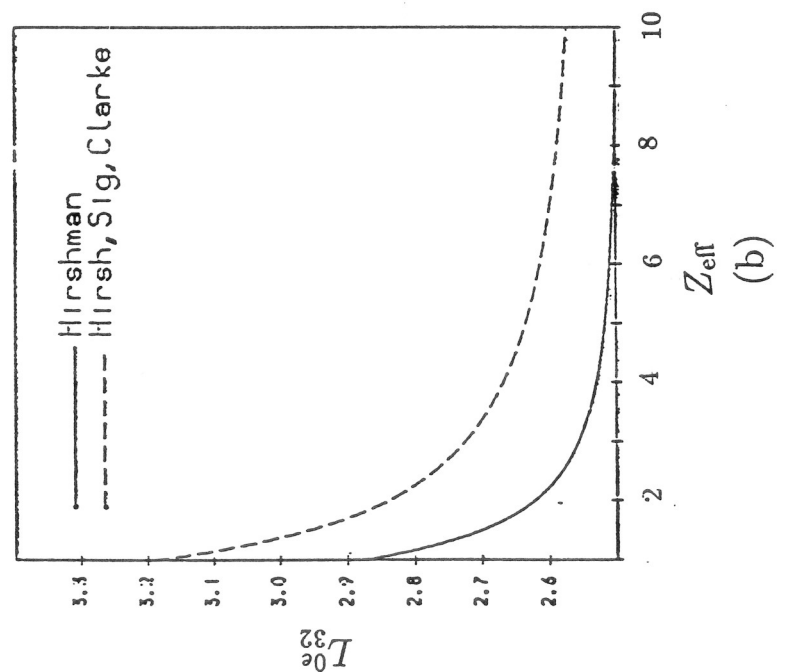
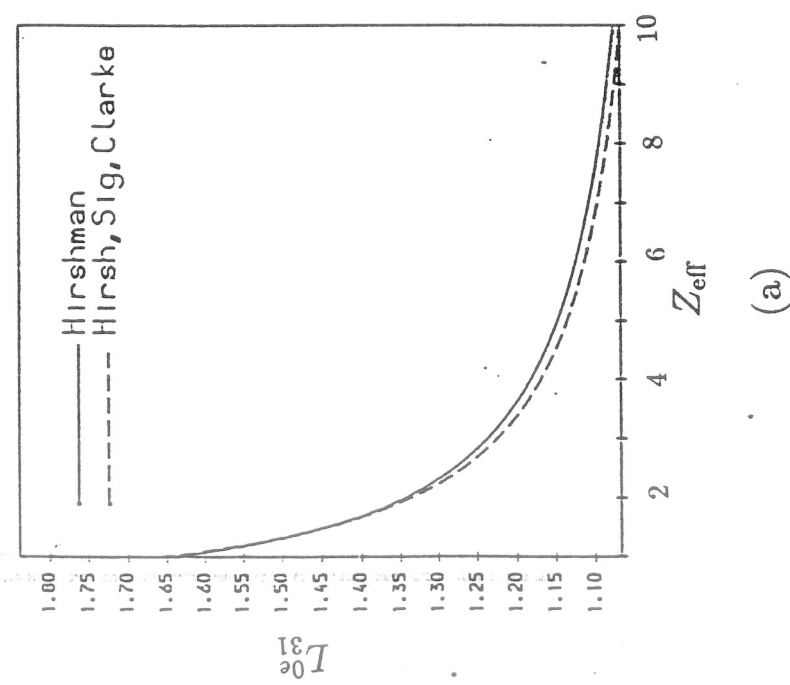


Figure 2a

SCENE 3.0 Test Case

Safety Factor

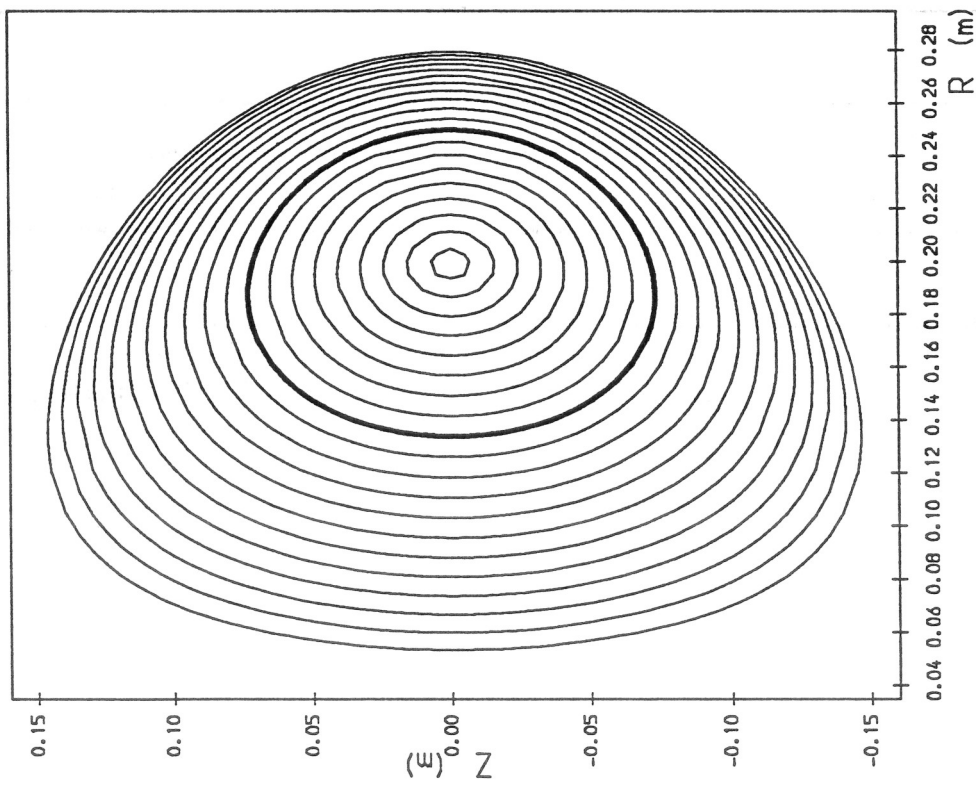
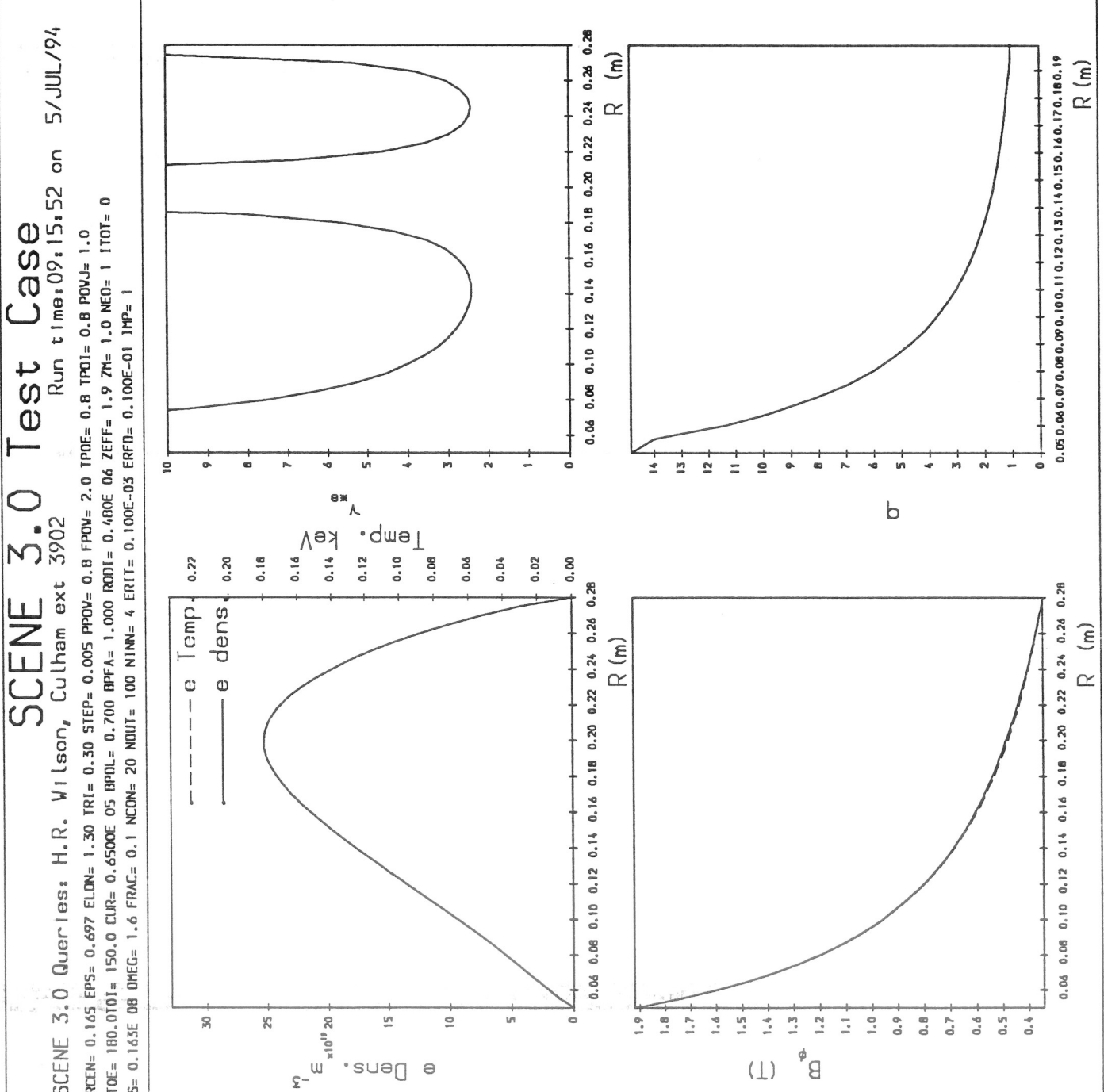


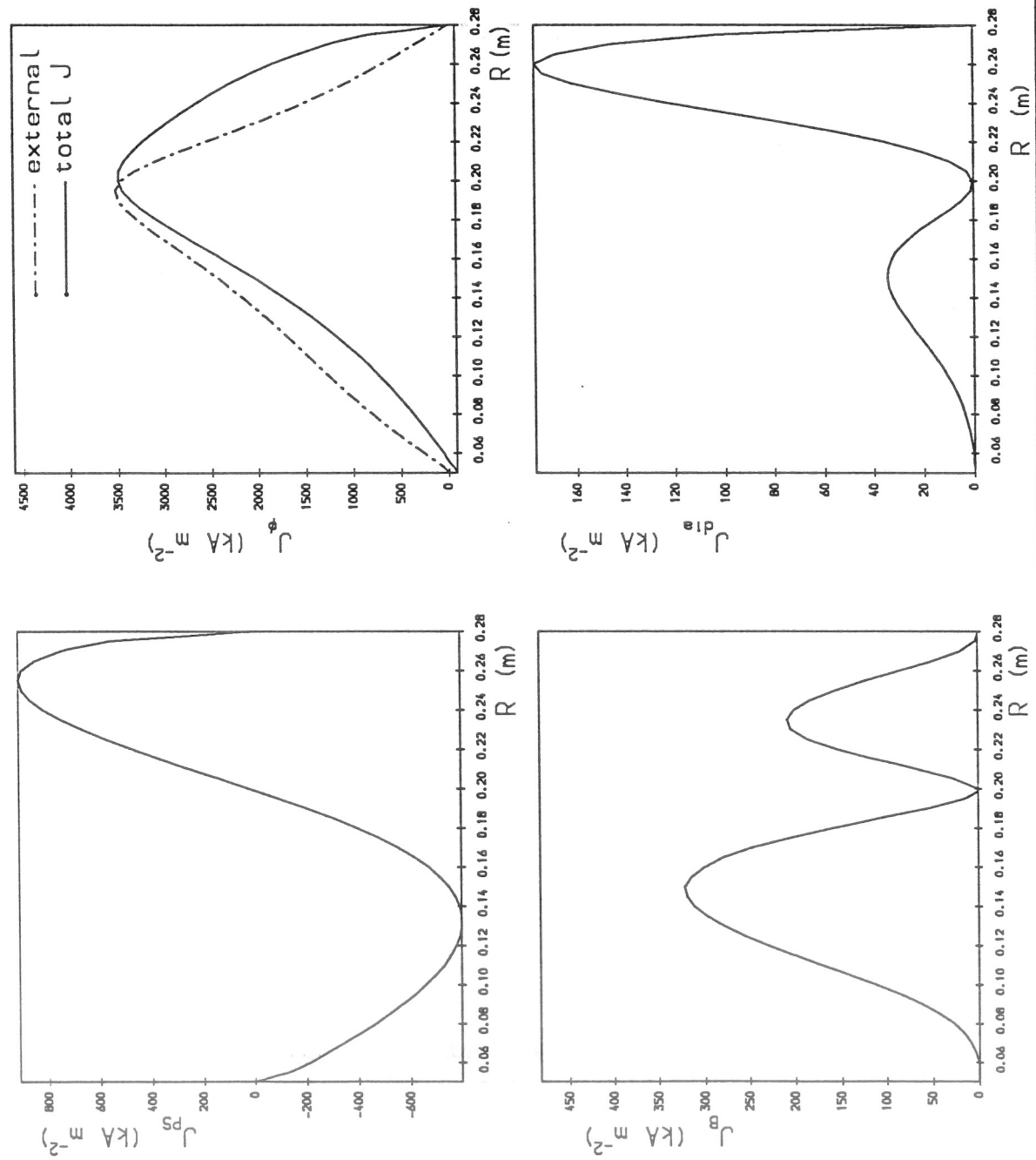
Figure 2b



## Parameters

Figure 2c

### SCENE 3.0 Test Case



### Parameters

Toroidal current=	0.0650 MA
Tor. b/s current=	0.0057 MA
Tor. p/s current=-0.0004 MA	
Tor. dia current=	0.0018 MA
Tor. ext. current=	0.0580 MA
Dimensionless $l_i$ =	0.7749
X sec area=	0.0538 $\text{m}^2$
$1.5 \int p dV$ =	0.0003 MJ
Loop voltage=	1.9645 V
Loop V ( $J_{bs}=0$ )	= 2.1567 V
Loop V (Spiltz.)	= 1.7479 V
Elongation=	1.300
Triangularity=	0.300
Aspect ratio=	1.435
Geometric axis=	0.165m
Rod I =	0.480MA